

Synthesis and Photochemical Behavior of Phosphorus Dendrimers Containing Azobenzene Units within the Branches and/or on the Surface

Rosa-María Sebastián,^[a] Jean-Claude Blais,^[b] Anne-Marie Caminade,*^[a] and Jean-Pierre Majoral*^[a]

Dedicated to all the victims of the explosion that occurred in Toulouse on September 21st, 2001.

Abstract: We describe the synthesis of three series of phosphorus-containing dendrimers having azobenzene derivatives specifically placed at some generations in the interior and/or on the surface. The largest compound obtained possesses 48 azobenzene groups on the surface. Irradiation at 350 nm induces isomerization of the azobenzene groups

from the *E* form to the *Z* form, whatever their location. The thermal back-isomerization to the *E* form in the dark at room temperature was observed in all cases.

Keywords: azo compounds • dendrimers • phosphorus • photochemistry

The kinetics of this *Z* → *E* back-isomerization was studied in several cases; the rate is not dependent on the number of azobenzene units or of the generation, when the azobenzene groups are linked to the surface of the dendrimer. A different behavior was observed when the azobenzene groups were located within the framework of the dendrimer.

Introduction

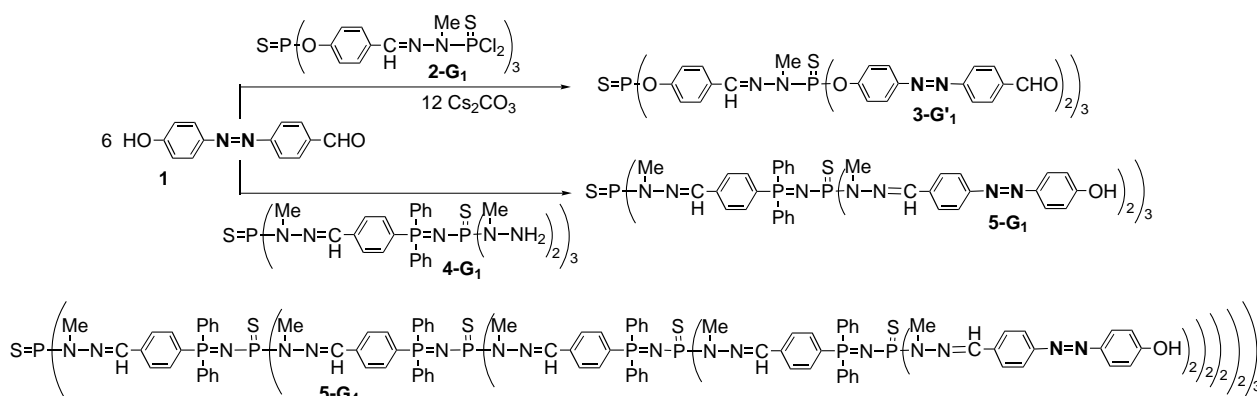
Dendrimers constitute an exciting class of special polymers, whose outstanding features attract intense interest. Indeed, these hyperbranched macromolecules synthesized in a step-wise iterative fashion have potential practical applications springing from their unusual architecture.^[1] Furthermore, dendrimers offer a unique opportunity for the study of physicochemical behavior of particular groups as a function of their number, their location, and the molecular size in well-defined macromolecules.^[2] It was shown that the properties of these macromolecules can correspond to a simple addition of the elementary properties, to a reduction in these properties, or to an increase (the so-called “dendritic effect”). These effects may result from the synergistic combination of the chemical constitution of the building blocks of the dendrimer and the reduced accessibility of the functional groups to be studied. In order to unify and rationalize these puzzling results and to free them from the influence of the nature of the building blocks, we decided a few years ago to study a single

family of dendrimers, easily tunable to place particular groups precisely within their structural interior or at their periphery.^[3] We have already demonstrated for these phosphorus-containing dendrimers that the value of a precise property divided by the number of groups concerned decreases for the dipole moment,^[4] is a constant for the chiroptical^[5] and electrochemical^[6] properties, and increases for the catalytic properties,^[7] the stabilization of naked Au₅₅ clusters,^[8] and the transfection efficiency,^[9] as a function of the generation. Pursuing this work, we thought it important to study the behavior and properties of photoactive moieties precisely placed within a dendrimer, which would undergo reversible photoinduced configurational changes. Azobenzene derivatives appear the most suitable photoactive moiety, since it is well known that they undergo an efficient and fully reversible photoisomerization reaction.^[10] Azobenzene groups have already been included in the skeleton of dendritic macromolecules either in the exterior,^[11] at the core,^[12, 13] throughout the dendritic architecture,^[14, 15] or at a precise generation,^[16] with various intentions. Among them, one can cite the encapsulation of guest molecules^[11c] and their transport,^[13a, 13b] optical switching,^[11b, 11c] holographic storage,^[11d] light harvesting,^[12a, 12b] long-term energy storage,^[12c] and nonlinear optical materials.^[15] Furthermore, their interesting properties for high-performance technological materials were recently emphasized.^[17]

We describe here the design of new dendritic structures having azobenzene derivatives precisely placed at some generations in the interior and/or at the surface. Figure 1 illustrates various generations of three types of dendrimers.

[a] Dr. A.-M. Caminade, Dr. J.-P. Majoral, Dr. R.-M. Sebastián
Laboratoire de Chimie de Coordination, CNRS
205 route de Narbonne, 31077 Toulouse Cedex 04 (France)
Fax: (+33) 5-61-55-30-03
E-mail: caminade@lcc-toulouse.fr, majoral@lcc-toulouse.fr

[b] Dr. J.-C. Blais
Laboratoire de Chimie Structurale Organique et Biologique
CNRS (UMR 7613)
Université Pierre et Marie Curie
4 Place Jussieu, 75252 Paris Cedex 05 (France)



Scheme 1. Synthesis of dendrimers with azo groups on the surface only.

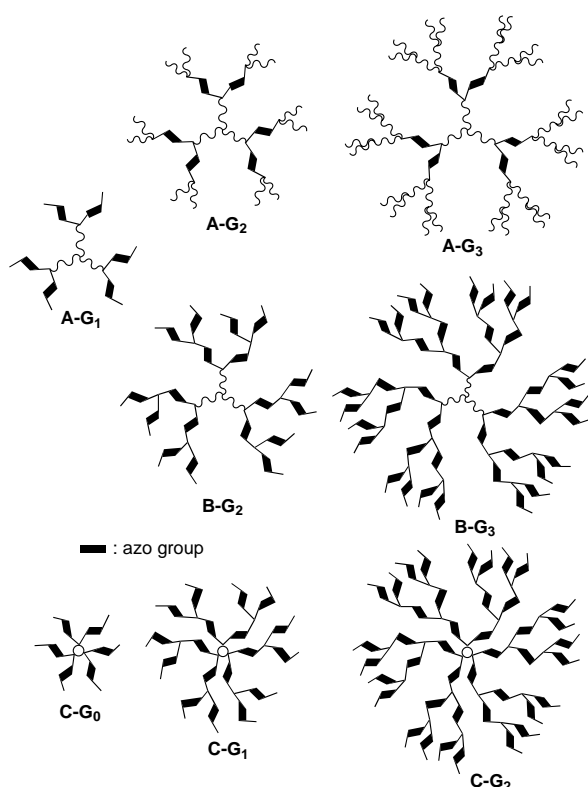


Figure 1. Various types of azobenzene-containing dendrimers.

Abstract in French: La synthèse de trois séries de dendrimères phosphorés ayant des dérivés de l'azobenzène placés spécifiquement à l'intérieur et/ou à la surface est décrite. Le plus grand composé obtenu possède 48 groupements azobenzène en surface. L'irradiation à 350 nm provoque l'isomérisation des groupements azobenzène de la forme *E* vers la forme *Z*, quelle que soit leur localisation. L'isomérisation thermique de retour vers la forme *E*, à température ambiante dans le noir, est observée dans tous les cas. La cinétique de cette isomérisation retour *Z* → *E* a été étudiée dans plusieurs cas; lorsque les groupes azobenzène sont greffés à la surface du dendrimère, la vitesse ne dépend pas de leur nombre, ni de la génération. Un comportement différent est observé lorsque les groupes azobenzène sont situés à l'intérieur de la structure du dendrimère.

The **A** family corresponds to azobenzene groups placed at the first generation and progressively buried in the interior when the dendrimer is grown. The **B** family corresponds to dendrimers having azobenzene groups at each generation (except at the very core, to avoid a large steric hindrance during isomerization). The **C** family corresponds to dendrimers having azobenzene groups at each generation starting from a hexafunctional core. Furthermore, the number of azobenzene groups is the same for dendrimers **A-G₁** and **C-G₀** (6), for **B-G₂** and **C-G₁** (18), and for **B-G₃** and **C-G₂** (42); this fact will allow comparison of the influence of crowding on the photochemical properties.

Results and Discussion

Syntheses: To build up dendrimers incorporating azobenzene groups precisely placed within their skeleton and using a procedure derived from the one we generally use,^[3] we need an analogue of *p*-hydroxybenzaldehyde. The unsymmetrical azobenzene derivative HO-C₆H₄-N=N-C₆H₄-CHO (**1**)^[18] appears the most suitable for this purpose. Furthermore, it can also be grafted onto the surface of a dendrimer, by means of either the phenol or the aldehyde function.

In our first attempt, we treated six equivalents of **1** with first-generation dendrimers. The reaction of the chloride derivative **2-G₁** in the presence of cesium carbonate affords dendrimer **3-G₁**, which has six azo and six aldehyde groups on the surface, while the reaction of the hydrazine derivative **4-G₁**^[19] affords dendrimer **5-G₁** with six azo and six phenol groups on the surface (Scheme 1). Of course, the grafting of functionalized azo derivatives could be extended to higher generation dendrimers, as illustrated by the fourth-generation **5-G₄**, possessing 48 azobenzene and 48 phenol groups. To the best of our knowledge, this is the largest number of azo groups linked to the surface of a dendrimer obtained so far.^[20]

The presence of reactive groups on the surface, particularly the aldehyde functions, permits the continuation of the synthesis of higher generations of dendrimers. Thus, compound **3-G₁** can be used as starting reagent, either for the synthesis of dendrimers having azo derivatives only in the interior at the level of the first generation (**A-G_n** family), or at each layer within the branches and on the surface (**B-G_n**,

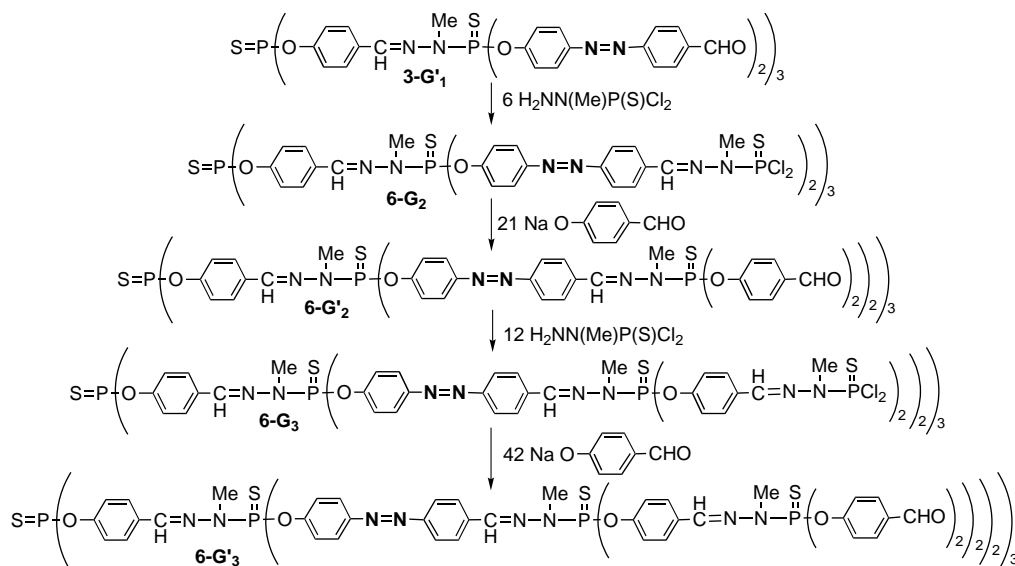
family). The former dendrimers are built from $\text{H}_2\text{NNMeP(S)Cl}_2$ and $\text{NaOC}_6\text{H}_4\text{CHO}$ alternately (Scheme 2), whereas the latter are built from alternate use of $\text{H}_2\text{NNMeP(S)Cl}_2$ and $\text{HOC}_6\text{H}_4\text{N}=\text{NC}_6\text{H}_4\text{CHO}$ in the presence of cesium carbonate (Scheme 3). In both cases, the synthesis is stopped at the third generation, giving dendrimers **6-G₃** and **7-G₃**, respectively. Both compounds possess 24 CHO end groups, but **6-G₃** has only six azo groups located at the level of the first generation, whereas **7-G₃** has 42 azo groups located in three layers, six at the level of the first generation, 12 at the second generation, and 24 at the third generation, that is, the surface.

Analogous reactions were carried out starting from a cyclotriphosphazene core. In this case, the azobenzene derivatives were directly grafted onto the core, leading to the hexaazo hexaaldehyde **8-G₀** (Scheme 4). Using the sequence of reactions already described for **7-G₃**, the synthesis was carried out up to the formation of the second generation **8-G₂** (**C-G_n** family). This dendrimer possesses

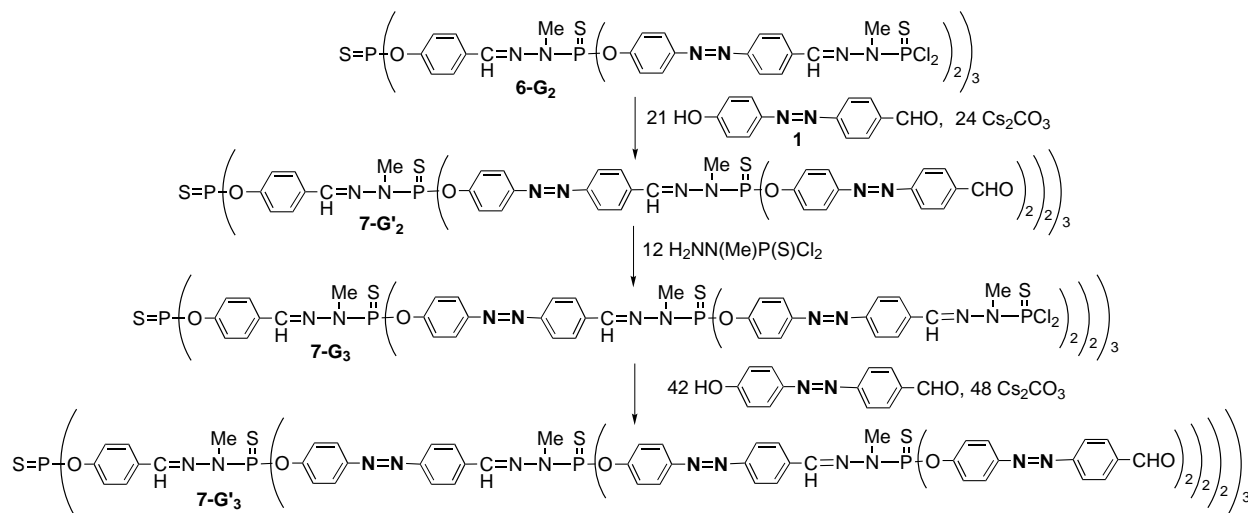
exactly the same number of azobenzene groups and aldehyde functions as **7-G₃**, but its synthesis requires two steps fewer than the preceding one.

Characterizations: All reactions were monitored by NMR spectroscopy, particularly by ^{31}P NMR spectroscopy for the $\text{P-Cl} \rightarrow \text{P-O-Ar}$ transformation (from $\delta \cong 63$ to $\delta \cong 61$) and ^1H NMR spectroscopy for the $\text{CHO} \rightarrow \text{CH=N-R}$ transformation (disappearance of the aldehyde signal at $\delta = 10$). Both techniques indicated complete reaction at each step with a precision better than 1%. Size exclusion chromatography gave thin traces for all dendrimers.

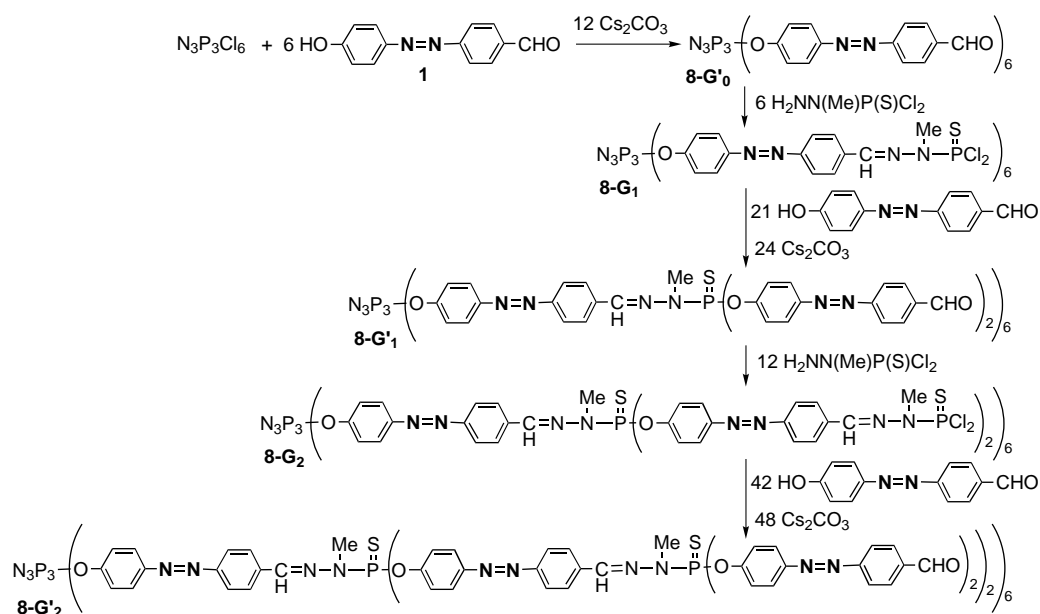
We also tried to characterize these dendrimers by MALDI-TOF mass spectrometry. We have already reported for dendrimers containing hydrazone moieties that fragmentations occur at the level of these bonds owing to their ability to absorb the laser energy.^[21] The presence of azo linkages could prevent this fragmentation, because the wavelength of the laser light (337 nm) is in a zone in which the azobenzene



Scheme 2. Synthesis of dendrimers with interior, first-generation azo groups only (**A-G_n** family).



Scheme 3. Synthesis of dendrimers with interior and surface azo groups (**B-G_n** family).



Scheme 4. Synthesis of C-G_n family of dendrimers in which the azobenzene derivative is grafted directly onto a core.

groups absorb strongly (see later). Thus, the expected *trans-cis* isomerization of the azobenzene bonds could help to release the laser energy and to keep the whole molecule intact. Initial experiments were carried out with $\mathbf{8-G'_0}$, which possesses six azo bonds but no hydrazone bond, in order to check the stability of the azo bonds. The experiments done with DHB as matrix were disappointing, since fragmentation of the azo bonds (multiple losses of 117 u) are observed (Figure 2a). However, the use of dithranol (1,8,9-anthracenetriol) as matrix gave much better results, and all fragmentations disappeared (Figure 2b). This trend is similar to the one observed for dendrimers containing hydrazone moieties.^[21] We tried to apply the same technique to $\mathbf{3-G'_1}$, which possesses both azo and hydrazone bonds. Fragmentation was observed at both levels (respective losses of 117 u and 541 u) when DHB was used as matrix (Figure 3a). Better results were obtained with dithranol as matrix, particularly if LiI was added (Figure 3b). However, fragmentation was still observed, even though a clean spectrum was obtained for the analogous compound without azo groups.^[21] In view of these findings, we predicted that the results should be worse with higher generations. Indeed, fragmentation was observed in these cases, in a dramatically higher proportion than that observed for analogous compounds without azo bonds,^[21] even if the molecular peak was observed. Thus, one may suppose that the azo bonds absorb energy but then partly transfer it to the hydrazone bonds, inducing their destabilization instead of protecting them. Consequently, MALDI-TOF MS cannot be used to characterize structure defects for these phosphorus- and azo-containing dendrimers.

Photochemical behavior: The UV–visible spectrum of azobenzene derivative **1** has one intense $\pi\pi^*$ band at $\lambda_{\text{max}} = 366 \text{ nm}$ ($\epsilon = 27000 \text{ M}^{-1} \text{ cm}^{-1}$) and a flat $n\pi^*$ band (Table 1). The $\pi\pi^*$ band of **1** is greatly red-shifted when compared with azobenzene ($\lambda_{\text{max}} = 318 \text{ nm}$), presumably because the elec-

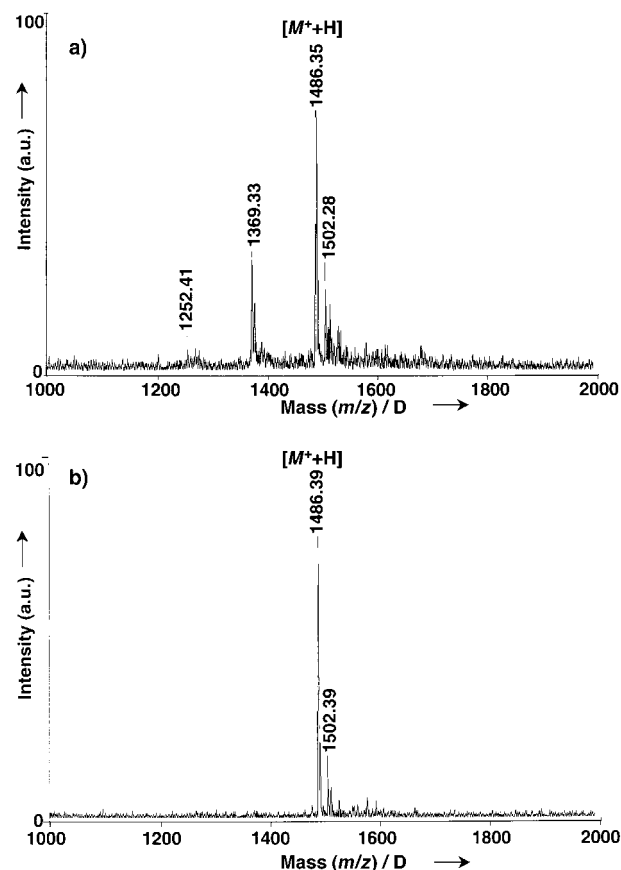
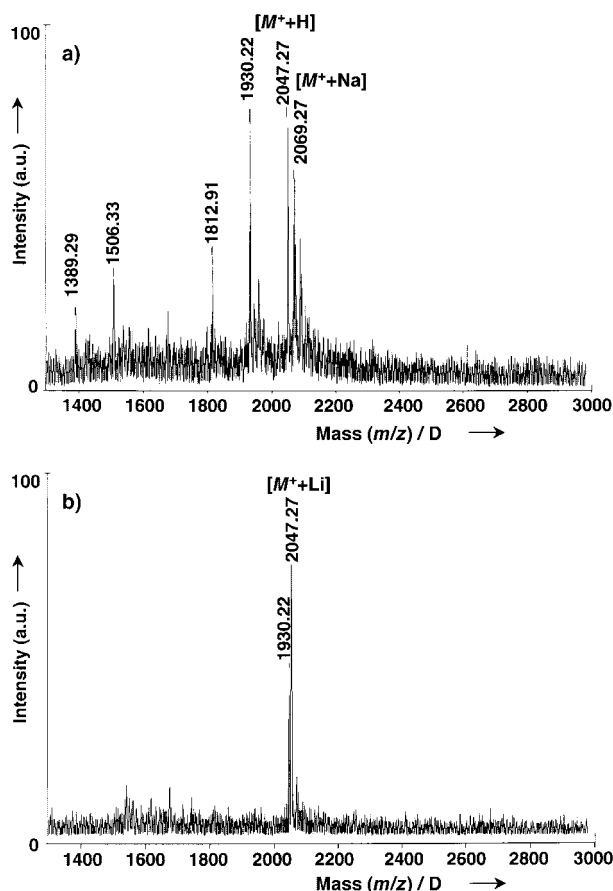


Figure 2. MALDI-TOF MS spectra of compound $\mathbf{8-G'_0}$. a) DHB as matrix. b) Dithranol as matrix.

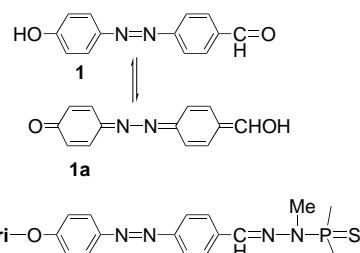
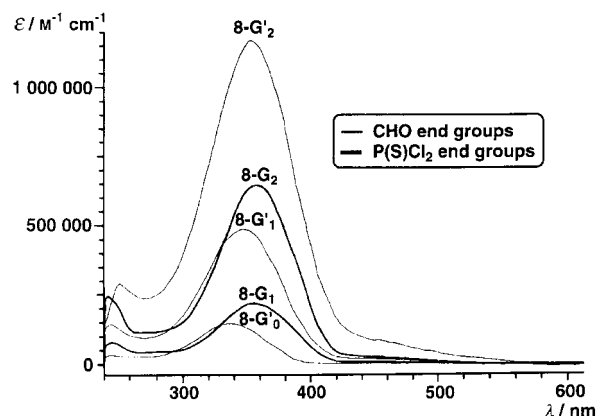
trons of **1** can be delocalized in the highly conjugated form **1a** (Scheme 5), which can no longer exist after the grafting of **1** to phosphorus. Thus, a large decrease is observed for the λ_{max} value of $\mathbf{8-G'_0}$ (336 nm; $\Delta\lambda = -30 \text{ nm}$) (Table 1, Figure 4). The condensation with the phosphorhydrazone leading to $\mathbf{8-G_1}$

Table 1. UV–visible spectroscopy data.

	No. of N=N	$\lambda_{\max} \text{ ArN=NAr}$ $\pi \rightarrow \pi^* \text{ [nm]}$	$\epsilon_{\text{ArN=NAr}}$ $\pi \rightarrow \pi^* \text{ [}^{\text{a}}\text{]} \text{ [M}^{-1} \text{ cm}^{-1}\text{]}$	$\epsilon/\text{No. N=N} \text{ [}^{\text{a}}\text{]}$	$\lambda_{\max} \text{ N=N}$ $n \rightarrow \pi^* \text{ [nm]}$	$\epsilon_{\text{N=N}}$ $n \rightarrow \pi^* \text{ [}^{\text{a}}\text{]} \text{ [M}^{-1} \text{ cm}^{-1}\text{]}$	$\lambda_{\max} \text{ other Ar}$ $\pi \rightarrow \pi^* \text{ [nm]}$	$\epsilon_{\text{other Ar}}$ $\pi \rightarrow \pi^* \text{ [}^{\text{a}}\text{]} \text{ [M}^{-1} \text{ cm}^{-1}\text{]}$
1	1	366	27 000	27 000	too flat			
3-G'₁	6	340	157 800	26 300	444	4100	290	124 300
6-G'₂	6	360	223 200	37 200	too flat		284	200 800
6-G'₂	6	362	198 600	33 100	442	10 100	258	269 700
6-G'₃	6	366	194 400	32 400	444	12 100	286	384 500
6-G'₃	6	366	204 000	34 000	too flat		262	525 400
7-G'₂	18	348	489 600	27 200	448	39 000		
7-G'₃	18	362	648 000	36 000	442	37 500		
7-G'₃	42	352	1 155 000	27 500	460	74 700		
8-G'₀	6	336	151 200	25 200	434	5 700		
8-G'₁	6	356	225 600	37 600	440	9 800		
8-G'₁	18	348	498 600	27 700	440	22 300		
8-G'₂	18	362	662 400	36 800	446	35 600		
8-G'₂	42	352	1 176 000	28 000				

[a] Estimated error on the molar absorption coefficient ϵ is $\pm 10\%$.Figure 3. MALDI-TOF MS spectra of compound **3-G'₁**. a) DHB as matrix. b) Dithranol as matrix, LiI added.

should lengthen the conjugation (Scheme 5). Indeed, we have shown several times by X-ray crystallography that $\text{O}-\text{C}_6\text{H}_4-\text{CH}=\text{N}-\text{N}(\text{Me})\text{P}=\text{S}$ linkages are flat, including the NMe group.^[3g-i, 4, 22] This trend is confirmed by the red shift observed on going from **8-G'₀** to **8-G'₁** ($\Delta\lambda = +20$ nm). The grafting of a second layer of azobenzene derivatives (compound **8-G'₁**) should give a composite band, made of both previously described influences. The final result is a slight decrease of the λ_{\max} value on going from **8-G'₁** to **8-G'₁**.

Scheme 5. Electron delocalization in **1** \rightleftharpoons **1a** and the lengthened conjugated compound **8-G'₁**.Figure 4. UV–visible spectra of dendrimers **8-G'₀**–**8-G'₂**.

($\Delta\lambda = -8$ nm). Analogous trends are observed for **8-G'₂** and **8-G'₂** (Table 1, Figure 4). As expected, the intensity of the $\pi\pi^*$ band increases with the number of azobenzene groups. An increase in this band is also observed with increasing conjugation for the same number of azobenzene groups, on going from **8-G'_n** to **8-G'_{n+1}**.

Different behavior is expected for the series **3-G'₁**, **6-G'₂**–**6-G'₃**. Indeed, the azobenzene-type units are not the only chromophoric groups for these dendrimers. Accordingly, another type of $\pi\pi^*$ band at a lower λ_{\max} value is expected, corresponding to the aryl aldehyde and/or aryl hydrazone groups. Indeed, compound **3-G'₁** exhibits two bands in the UV region at $\lambda_{\max} = 340$ nm for the azobenzene aldehyde groups and another band at $\lambda_{\max} = 290$ nm for the aryl hydrazone

groups (Table 1, Figure 5). Condensation with the phosphorhydrazide to afford **6-G₂** caused a red shift in the λ_{max} value of the $\pi\pi^*$ azobenzene band as expected ($\Delta\lambda = +20$ nm), but had little influence on the λ_{max} value of the other $\pi\pi^*$ aromatic band. The λ_{max} value and the intensity of the $\pi\pi^*$ azobenzene

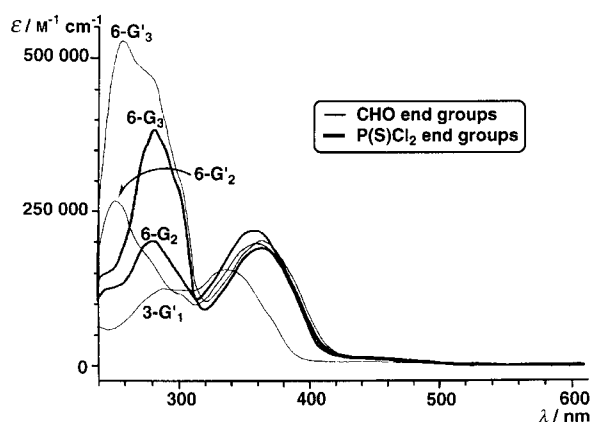


Figure 5. UV–visible spectra of dendrimers **3-G₁'**, **6-G₂**–**6-G₃'**.

band do not vary significantly on going up to the third generation **6-G₃'**, whereas they do for the other aromatic groups. The grafting of aryl aldehydes on **6-G₂**, leading to **6-G₂'**, induced a band to appear at a lower λ_{max} value (258 nm), with a shoulder due to the internal aryl hydrazones. Condensation with the phosphorhydrazide leading to **6-G₃** induced the expected red shift, affording a band at $\lambda_{\text{max}} = 286$ nm, which corresponds to the superposition of the signal of all the aryl hydrazones. Comments similar to those made for **6-G₂'** can be applied to **6-G₃'**.

Several conclusions can be inferred from these data. Study of the **3-G₃**, **6-G₂**–**6-G₃'** series demonstrates that the only factor influencing the wavelength and the intensity of the maximum of the $\pi\pi^*$ absorption band of the azobenzene derivative is the conjugation (see the transformation **3-G₁'** → **6-G₂**). Indeed, the growth of several layers without azo groups on this azo layer, progressively burying the azobenzene groups, had practically no influence on the λ_{max} value. The effects of conjugation on the λ_{max} value were also confirmed by studying the **8-G₀**–**8-G₂'** series. The value of the molar absorption coefficient increases with the number of azobenzene groups in a simple additive way. Indeed, it can be deduced from Table 1 that each azobenzene aldehyde group contributes $\approx 26000 \text{ M}^{-1} \text{ cm}^{-1}$ to the ϵ value, whereas each azobenzene–hydrazone group contributes for ≈ 37000 (hydrazone–P(S)Cl₂) or $\approx 34000 \text{ M}^{-1} \text{ cm}^{-1}$ (hydrazone–P(S)(OAr)₂) to the ϵ value. However, the difference between the two types of azobenzene–hydrazone groups may be not significant, since it lies within the limits of the precision of detection ($\pm 10\%$).

Thus, the position of a particular azobenzene group within the dendrimer has no influence upon its absorption properties. On the other hand, it must not be deduced from these findings that the isomerization properties will be identical for all compounds. In order to study the influence of the location upon the isomerization properties of the N=N groups, we

decided to perform some kinetic experiments. However, the sensitivity of dendrimers **3** and **5–8** toward laser irradiation observed in mass spectrometry could preclude any study concerning the photoinduced configurational changes of their azobenzene moieties. Thus, our first concern was to verify the stability of the dendrimers in the conditions used for the $E \rightarrow Z$ isomerization of the azobenzene moieties.

Irradiations were carried out at 350 nm, that is, in the $\pi\pi^*$ band of the azobenzene moieties of the dendrimers, in chloroform, with concentrations suitable for NMR experiments. Only dendrimers with aldehyde end groups were studied, and we focused most of our work on dendrimers **3-G₁'**, **6-G₂'**, **7-G₂'**, and **8-G₀'**. After several hours of irradiation of the dendrimers (3 to 24 h), new peaks appear in the ³¹P NMR spectra close to the peaks corresponding to the initial dendrimers. ¹H NMR spectra show complicated patterns in the aromatic region, but the aldehyde signal provides very useful information. Indeed, in all cases it is a singlet for the initial all-*trans* dendrimers. After irradiation, new signals slightly shielded appear in the aldehyde region. The shielding is $\Delta\delta = 0.2$ ppm when the aldehyde is directly linked to the azobenzene group, namely, for **3-G₁'** (Figure 6a). Keeping this

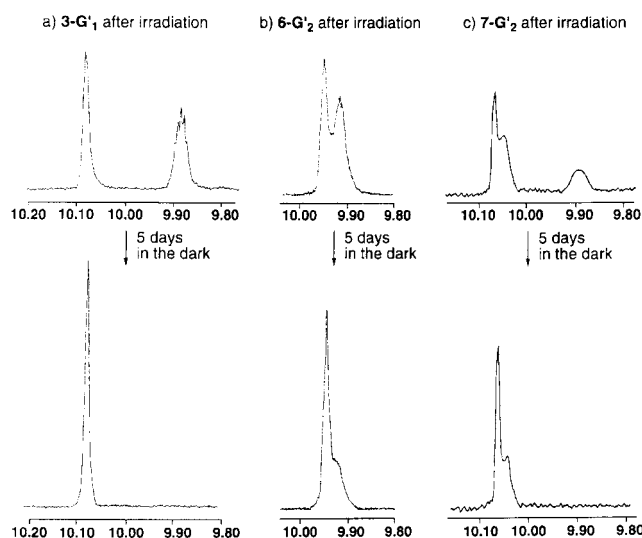


Figure 6. Evolution of the aldehyde signals in ¹H NMR spectra after irradiation at 350 nm.

solution in the dark at 20 °C allows the total recovery of the initial aldehyde singlet in ¹H NMR spectrum, and the ³¹P NMR spectrum corresponds again to the all-*trans* initial dendrimer. Surprisingly, a shielding of the aldehyde signal is also observed when the aldehyde is located 14 bonds away from the azo group (**6-G₂'**). The shielding is smaller ($\Delta\delta = 0.035$ ppm) but easily detectable (Figure 6b). When this solution is kept in the dark for five days and then examined by ¹H NMR spectroscopy, the signal corresponding to the presence of *cis* isomers is diminished, but it does not disappear totally. Thus, the rate of the recovery of the *trans* form seems to be slower for **6-G₂'** than for **3-G₁'**. However, the recovery of the all-*trans* dendrimer was total after a few weeks.

Dendrimer **7-G'**₂ possesses azo derivatives at two levels; thus it is expected that irradiation will induce the formation of *cis* isomers at both levels, creating combinatorial series. We thought that only modifications of the external azo groups could be detected in ¹H NMR spectra, but very unexpectedly, three signals are observed for the aldehyde groups after irradiation (Figure 6c). Besides the signal corresponding to the initial *trans*-azoaldehyde groups, a signal very close ($\Delta\delta = 0.015$ ppm) and a broad, more shielded signal ($\Delta\delta = 0.200$ ppm) appear. The only way to account for these results is to consider that the isomerization of the internal groups is also detectable in ¹H NMR spectra, even if this isomerization occurs 20 bonds away from the aldehyde end groups. Thus, the most deshielded (initial) signal corresponds to *trans*-azoaldehydes pertaining to [*trans*-N=N_(CHN)-(*trans*-N=N_(CHO))₂] and [*trans*-N=N_(CHN)-(*cis*-N=N_(CHO))(*trans*-N=N_(CHO))] branches, the signal closest to this one corresponds to *trans*-azoaldehydes pertaining to [*cis*-N=N_(CHN)-(*trans*-N=N_(CHO))₂] and [*cis*-N=N_(CHN)-(*cis*-N=N_(CHO))(*trans*-N=N_(CHO))] branches, and the most shielded signal corresponds to *cis*-azoaldehydes pertaining to [*trans*-N=N_(CHN)-(*cis*-N=N_(CHO))₂], [*cis*-N=N_(CHN)-(*cis*-N=N_(CHO))₂], [*trans*-N=N_(CHN)-(*trans*-N=N_(CHO))-(*cis*-N=N_(CHO))], and [*cis*-N=N_(CHN)-(*trans*-N=N_(CHO))-(*cis*-N=N_(CHO))] branches (Figure 7). The presence of four

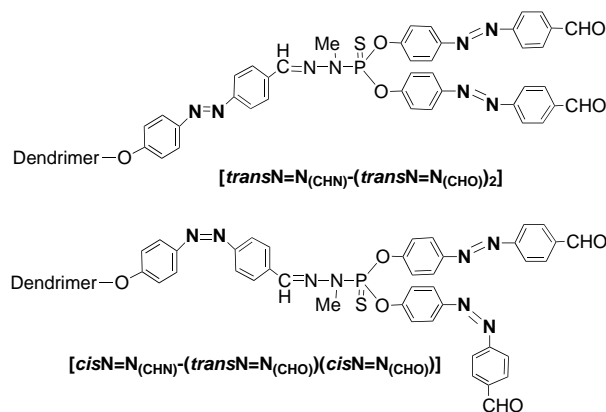


Figure 7. Examples of branch isomerism.

types of isomers within this last signal may account for its broadening when compared to the others. Keeping this solution in the dark for five days induced the phenomena already observed for **3-G'**₁ and **6-G'**₂. The signal corresponding to the external *cis*-azo groups disappeared, whereas the signal corresponding to the internal *cis*-azo groups diminished but did not disappear, indicating a different rate for the recovery of the *trans* form. However, the all-*trans* form reappeared after several weeks in the dark. Some of these solutions, in particular those containing dendrimers **3-G'**₁ and **8-G'**₀, were reirradiated and back-isomerized several times (up to seven times) to check their stability over time. No decomposition could be detected by comparing the data furnished by NMR techniques and size exclusion chromatography (SEC) of the irradiated products (after recovery of the all-*trans* form) with those of nonirradiated samples.

These first experiments reassured us of the stability of these azobenzene dendrimers towards irradiation in the conditions used for the isomerization. Thus, we decided to study the photochemical behavior of several azobenzene-containing dendrimers described in this paper, mostly those having aldehyde end groups. The experiments were carried out at 295 K in CH₂Cl₂ or CHCl₃, no difference being observed between experiments carried out in one or the other solvent. In all cases, the *E* → *Z* photoisomerizations were observed by UV–visible spectroscopy. As an example, Figure 8 displays

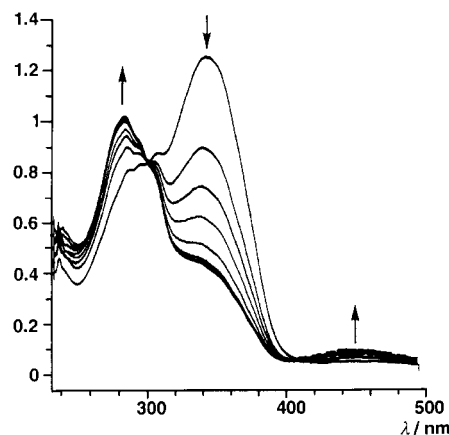


Figure 8. Changes in the UV–visible spectrum of **3-G'**₁ upon irradiation at 350 nm.

the spectral changes observed for the *E* → *Z* photoisomerization of compound **3-G'**₁ under 350 nm light. As expected, an important decrease of absorbance was observed in the near-UV spectral region ($\pi\pi^*$ absorption band) whereas a slight increase was observed in the visible region ($n\pi^*$ absorption band). The presence of isosbestic points during isomerization confirms the independence of each chromophoric unit. After a few minutes, the photostationary equilibrium was reached in dilute solutions ($c_{\text{azo}} \cong 10^{-5}$ M), but several hours were needed for concentrated solutions ($c_{\text{azo}} \cong 10^{-3}$ M). Assuming that the absorbance of the *Z* isomer at the wavelength of the $\pi\pi^*$ band maximum can be neglected,^[11d] the relative amount of *E* and *Z* isomers can be deduced from the value of the absorbance at the photostationary equilibrium (Table 2). In some cases, the *E/Z* ratio was directly measured by ¹H NMR spectroscopy

Table 2. Photostationary equilibria and kinetic data for thermal back-isomerization (*Z* → *E*).

	No. N=N	Photostationary eq. <i>Z</i> [%] ^[a]	k_{295} [s ⁻¹]	Method
1	1	67	9×10^{-4}	UV/Vis
3-G' ₁	6	63	1.5×10^{-5}	¹ H NMR
6-G' ₂	6	52		
6-G' ₂	6	52	3.3×10^{-6}	¹ H NMR
6-G' ₃	6	42		
7-G' ₂	18	30	1.3×10^{-5} ^[b]	¹ H NMR
7-G' ₃	42	21		
8-G' ₀	6	47	1.4×10^{-5}	¹ H NMR
8-G' ₁	6	44		
8-G' ₂	42	12		

[a] For dilute solutions. [b] For azo groups at the surface only.

and correlated well with the values deduced from UV absorption, confirming the assumption made previously on the negligible value of the *Z* absorption. Interesting conclusions can be drawn from these data. First, the progressive burying of the azobenzene groups inside the dendrimer induces a progressive reluctance of the azobenzene groups to isomerize, as shown by the decreasing amount of *Z* form registered on going from **3-G**₁' to **6-G**₃', from 63 % to 42 % of *Z* isomer. Second, a higher density also induces a lower percentage of isomerization, as shown by the comparison between **3-G**₁' and **8-G**₀' (63 % and 47 % of *Z* isomer, respectively), or between **7-G**₃' and **8-G**₂' (21 % and 12 % of *Z* isomer, respectively). Third, a higher number of azobenzene groups also induces reluctance of the azo groups to isomerize, as shown by the comparison between **6-G**₃' and **7-G**₃' (42 % and 21 % of *Z* isomer, respectively).

The NMR data indicate that the thermal back-isomerization (*Z* → *E*) is a rather lengthy process for dendrimers (several hours to several days). We could not use UV–visible spectrophotometry to study these kinetics, owing to problems of temperature regulation over a long time inducing unreliable results. The only usable UV–visible kinetic data concerned compound **1** in dilute solutions ($c = 4.4 \times 10^{-5}$ M), which back-isomerizes in the dark within less than one hour. The t_0 time corresponds to the end of irradiation. A plot of $\ln(A - A_0)$ versus time is a straight line, with A_0 being the absorbance at 359 nm (λ_{\max}) for the *trans* isomer, and A being the absorbance at 359 nm at time t (Figure 9). The slope gives the value of the first-order rate constant, $k = 9 \times 10^{-4} \text{ s}^{-1}$ at 295 K (Table 2). Because of the high rate of isomerization, we could not monitor it by ^1H NMR spectroscopy.

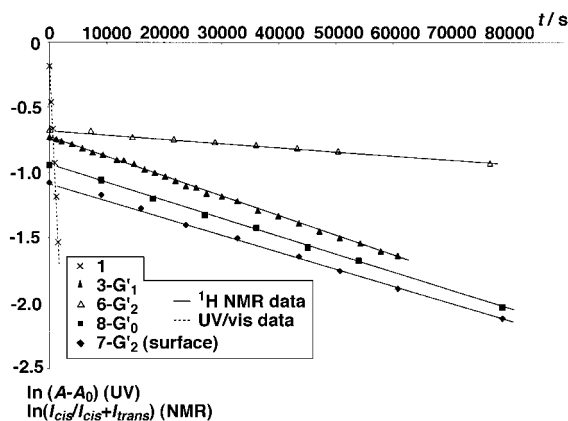


Figure 9. Kinetic data for the thermal back-isomerization (*Z* → *E*) of the azo bonds for compounds **1**, **3-G**₁', **6-G**₂', **8-G**₀', and the surface azo groups of **7-G**₂'.

On the other hand, ^1H NMR spectroscopy is a perfectly suitable technique to monitor the *Z* → *E* isomerization of azo dendrimers by integration of the signals corresponding to the aldehyde groups. This technique gives a direct measurement, which does not necessitate any approximation, unlike UV measurements. Concentrated solutions irradiated for several hours were used, but the photostationary equilibrium observed for dilute solutions was not reached in these cases, presumably because of differences in the temperature of the

samples during prolonged irradiation. The t_0 time was at least one hour after the end of irradiation, to allow the sample to reach a constant temperature (295 K) in the NMR machine. First experiments were carried out with dendrimer **3-G**₁'. A plot of $\ln[I_{\text{cis}}/(I_{\text{cis}} + I_{\text{trans}})]$ versus time was also a straight line, with I_{cis} and I_{trans} being the integration corresponding to the CHO groups linked to *cis* and *trans* azobenzene groups, respectively. The strict adherence to first-order kinetics demonstrates that all the azobenzene groups of dendrimer **3-G**₁' behave independently, as has already been demonstrated for other azo-containing dendrimers.^[16] The value of the first-order rate constant deduced from the slope is $k = 1.5 \times 10^{-5} \text{ s}^{-1}$ at 295 K (Table 2).

Analogous experiments were carried out with dendrimer **8-G**₀'. Its behavior is very similar to that observed for **3-G**₁', as expected for compounds having the same number of azo groups (i.e., six) located in the external layer. The first-order rate constant is $k = 1.4 \times 10^{-5} \text{ s}^{-1}$ (Figure 9, Table 2). On the other hand, dendrimer **6-G**₂' behaves differently. This compound derives from **3-G**₁' and it possesses the same number of azo groups (i.e., six), but they are included within the skeleton of the dendrimer and not on the surface. However, the same procedure can be applied to the ^1H NMR spectra of **6-G**₂', using integration of the aldehyde groups located on the surface at 14 bonds from the *trans* or *cis* azo groups. A straight line is also obtained when $\ln[I_{\text{cis}}/(I_{\text{cis}} + I_{\text{trans}})]$ is plotted versus time, indicating here also the independent behavior of the azo groups within the dendrimer. However, the rate constant k deduced from the slope is appreciably different: $3.3 \times 10^{-6} \text{ s}^{-1}$ for **6-G**₂' versus $1.5 \times 10^{-5} \text{ s}^{-1}$ for **3-G**₁' (Figure 9, Table 2).

Dendrimer **7-G**₂' constitutes a more complex case, owing to the presence of two types of azo derivatives, one type located on the surface and the other within the interior. The total description of the kinetic parameters of this system is not obtainable by ^1H NMR spectroscopy, but the rate of the *Z* → *E* isomerization of the azoaldehyde groups on the surface is accessible, again from a plot of $\ln[I_{\text{cis}}/(I_{\text{cis}} + I_{\text{trans}})]$ versus time. In this case, the I_{cis} value corresponds to the integration of the most shielded aldehyde signal, and the I_{trans} value corresponds to the sum of integration of the two most deshielded aldehyde signals (see above for the description of the attribution made for these signals, and Figure 6). The rate constant of the back-isomerization of the azoaldehyde groups is deduced from the straight line obtained in Figure 9, that is, $1.3 \times 10^{-5} \text{ s}^{-1}$.

Several conclusions can be drawn from these kinetic data. First, the *E* form of the azo groups located on the surface is recovered at identical rates whatever the generation considered (compare values obtained for **8-G**₀', **3-G**₁', and **7-G**₂'). Second, the burying of the azo groups within the dendrimeric structure (as in the case of **6-G**₂') considerably lowers the rate of the back-isomerization. At first glance, this result could be interpreted as the effect of steric hindrance and lower flexibility. However, it was previously demonstrated that the incorporation of azobenzene derivatives within dendrimers^[16] or polymers^[23] in fact has no influence upon their *cis*–*trans* thermal isomerization, even if a recent paper points out that the rate constant of this isomerization increases with the ring size for azobenzene-containing macrocycles.^[24] On the other hand, it is evident that the azo groups located on the surface

are of a type different from the azo groups located in the interior, with an aldehyde as substituent in the first case and a hydrazone in the second case. A difference in the substituents is known to induce a difference in the rate of the thermal isomerization.^[25] Another illustration of this behavior is given here by the large decrease observed between the azo derivative **1** (HO substituent) and the same azo derivative linked to the surface of the dendrimer (P–O substituent), for which steric hindrance is unlikely to be involved. Thus, it appears that a large part of the rate difference observed for the back-isomerization is most likely due to substituent effects rather than to position inside the dendrimer or on the surface.

Conclusion

We have synthesized three series of phosphorus-containing dendrimers with azobenzene units precisely placed within their framework. The presence of these azobenzene groups induces higher sensitivity of the dendrimer to laser light for the MALDI-TOF MS technique, but does not preclude studying the photochemical behavior of these dendrimers. The position of a particular azobenzene group within the dendrimer has no influence upon its absorption properties. The only factor influencing the wavelength of the maximum of the $\pi\pi^*$ absorption band is the conjugation, since the progressive burying of the azobenzene groups inside the dendrimer has practically no influence on the λ_{\max} value (series **3-G'**, **6-G**–**6-G'**). Furthermore, the value of the molar absorption coefficient ϵ_{\max} increases with the number of azobenzene groups in a simple additive way, within the limits of precision.

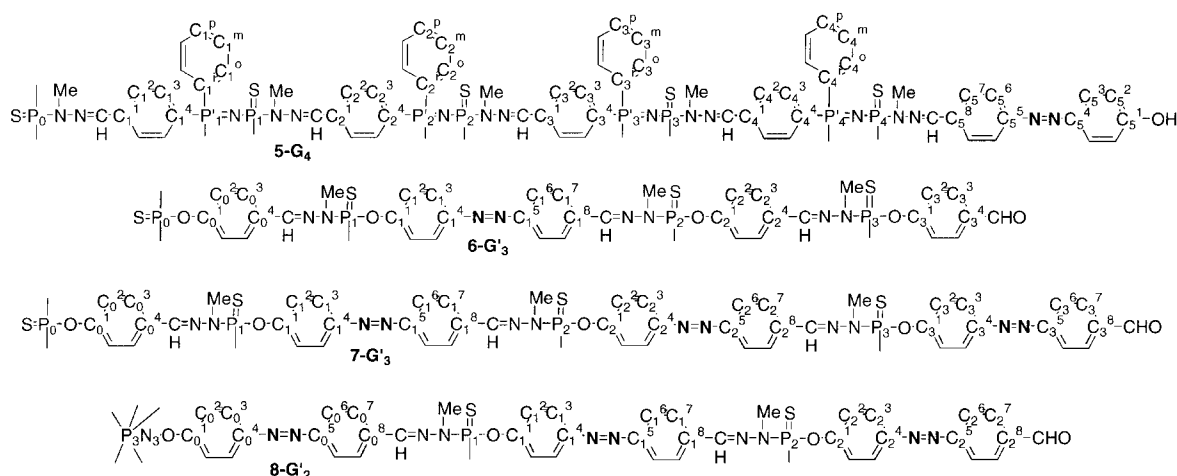
On the other hand, the relative amount of *E* and *Z* isomers obtained at the photostationary equilibrium reached by irradiation with a 350 nm light differs greatly depending on the location of the azobenzene groups. Progressive burying of the azobenzene groups inside the dendrimer induces a progressive reluctance to isomerize. A higher density and a higher number of azobenzene groups induce the same phenomenon. The kinetic data for the back-isomerization (*Z* → *E*) of some dendrimers was deduced from ¹H NMR

spectra. Very unexpectedly, it was shown that the signal corresponding to the aldehyde end groups is sensitive to configurational changes occurring at a distance of 14 and even 20 bonds from this group. A strict adherence to first-order kinetics is observed, demonstrating that all the azobenzene groups behave independently. The rate of recovery of the *E* form for azobenzene groups located on the surface is similar, whatever the generation—and thus the number of azobenzene groups—considered. On the other hand, the large difference observed for this rate depending on the location of the azobenzene groups appears most likely to be due to a substituent effect than to the location. Thus, surprisingly, the photochemical behavior of azobenzene groups is very comparable to the electrochemical behavior of ferrocene groups linked to or included in the same type of dendrimers.

Experimental Section

General: All reactions were carried out in the absence of air, by means of standard Schlenk techniques and vacuum-line manipulations. All solvents were dried before use. Instrumentation: Bruker AM250 and DPX300 (¹H, ¹³C, and ³¹P NMR); Perkin–Elmer 1725 X (FT-IR); Hewlett Packard (UV/Vis) connected to Hewlett Packard Vectra VL series 5/133 computer (program used: HP UV/Vis Configuration Edition); PerSeptive Biosystems Voyager Elite equipped with a nitrogen laser (337 nm) (mass spectrometry). All irradiation was carried out at 263 K with a homemade irradiation system equipped with 350 nm lamps. SEC data were obtained with a Waters 410 differential refractometer. The numbering used for NMR data of dendrimers is depicted in Scheme 6. References for NMR chemical shifts were 85 % H₃PO₄ for ³¹P NMR, SiMe₄ for ¹H and ¹³C NMR. The ¹³C NMR signals were assigned by *J*_{mod}, two-dimensional HMBC, and HMQC, broadband, or CW ³¹P decoupling experiments when necessary. Compounds **1**^[8] and **4-G**_n^[19] were prepared according to published procedures. All dendrimers containing azobenzene groups were protected against light at all times during the synthesis and were stored in the dark. Most photochemical experiments were carried out with several batches, without noticeable changes.

General procedure for the synthesis of dendrimers with azobenzene aldehyde end groups (3-G₁, 7-G₂, 7-G₃, 8-G₀, 8-G₁, 8-G₂): A mixture of dendrimer with P(S)Cl₂ end groups (*a*: **2-G**₁, 0.50 g, 0.55 mmol; *b*: **6-G**₂, 0.25 g, 0.083 mmol; *c*: **7-G**₃, 0.23 g, 0.032 mmol; *d*: N₃P₃Cl₆, 0.50 g, 1.44 mmol; *e*: **8-G**₁, 0.50 g, 0.204 mmol; *f*: **8-G**₂, 0.52 g, 0.078 mmol), 4-[(4-hydroxyphenyl)azo]-benzaldehyde (**1**; *a*: 0.77 g, 3.41 mmol; *b*: 0.23 g, 1.02 mmol; *c*: 0.18 g, 0.777 mmol; *d*: 2.00 g, 8.77 mmol; *e*: 0.57 g, 2.51 mmol; *f*: 0.43 g, 1.90 mmol), and Cs₂CO₃ (*a*: 2.22 g, 6.82 mmol; *b*:



Scheme 6. Numbering used for NMR studies.

0.67 g, 2.04 mmol; *c*: 0.51 g, 1.56 mmol; *d*: 5.60 g, 17.3 mmol; *e*: 1.63 g, 5.02 mmol; *f*: 1.24, 3.80 mmol) in THF (15–25 mL) was stirred overnight at room temperature, then evaporated to dryness. The residue was extracted with CH₂Cl₂ (3 × 25 mL). The liquid phases were recovered and evaporated under vacuum to give a paste, which was washed three times with THF/pentane (1/10) to give an orange powder of *a*: **3-G₁**; *b*: **7-G₂**; *c*: **7-G₃**; *d*: **8-G₀**; *e*: **8-G₁**; *f*: **8-G₂**.

General procedure for the synthesis of dendrimers 5-G_n (*n*=1, 4): One equivalent of dendrimer **4-G_n** (*n*=1: 0.200 g, 0.132 mmol; *n*=4: 0.098 g, 0.0049 mmol) and 3 × 2^{*n*} equivalents the azo derivative **1** (*n*=1: 0.18 g, 0.792 mmol; *n*=4: 0.053 g, 0.236 mmol) were dissolved in THF (*n*=1: 10 mL; *n*=4: 5 mL) and stirred overnight at room temperature. The solution was concentrated (2/3 of the solvent was evaporated), then pentane was added to precipitate a powder. The solution was filtered, and the powder was washed with THF/pentane (1/10) to give **5-G_n** as orange powders.

General procedure for the synthesis of dendrimers with P(S)Cl₂ end groups (6-G₂, 6-G₃, 7-G₃, 8-G₁, 8-G₂): A solution of Cl₂P(S)NCH₃NH₂ (0.23 mL) in CHCl₃ (*a*: 11.4 mL, 2.63 mmol; *b*: 3.10 mL, 0.714 mmol; *c*: 2.7 mL, 0.629 mmol; *d*: 7.0 mL, 1.60 mmol; *e*: 5.43 mL, 1.25 mmol) was added slowly to a solution of dendrimer with aldehyde end groups (*a*: **3-G₁**, 0.80 g, 0.390 mmol; *b*: **6-G₂**, 0.23 g, 0.0567 mmol; *c*: **7-G₂**, 0.26 g, 0.050 mmol; *d*: **8-G₀**, 0.36 g, 0.244 mmol; *e*: **8-G₁**, 0.47 g, 0.0992 mmol) in THF (5–20 mL) at room temperature. The resulting solution was stirred overnight, then the solvent was removed under vacuum, and the residue was washed three times with CH₂Cl₂/pentane (1/10) to give an orange powder of *a*: **6-G₂**, *b*: **6-G₃**, *c*: **7-G₃**, *d*: **8-G₁**, *e*: **8-G₂**.

General procedure for the synthesis of dendrimers with benzaldehyde end groups (6-G_n, *n*=2, 3): NaOC₆H₄CHO (*n*=2: 0.18 g, 1.24 mmol; *n*=3: 0.16 g, 1.12 mmol) was added to a solution of dendrimer **6-G_n** (*n*=2: 0.30 g, 0.0995 mmol, *n*=3: 0.28 g, 0.0462 mmol) in THF (15 mL). The resulting mixture was stirred overnight, then centrifuged and filtered. The solution was evaporated to dryness, and the residue was washed three times with THF/pentane (1/10) to give **6-G_n** as an orange powder.

Dendrimer 3-G₁: 98% yield (1.10 g); ³¹P {¹H} NMR (CDCl₃): δ = 52.6 (P₀), 61.3 (P₁); ¹H NMR (CDCl₃): δ = 3.43 (d, ³J(H,P) = 10.7 Hz, 9H; CH₃NP₁), 7.31 (dd, ³J(H,H) = 8.6 Hz, ⁴J(H,P) = 1.3 Hz, 6H; C₂H), 7.41 (dd, ³J(H,H) = 8.8 Hz, ⁴J(H,P) = 1.4 Hz, 12H; C₂H), 7.69 (s, 3H; CH=N₍₀₎), 7.76 (d, ³J(H,H) = 8.6 Hz, 6H; C₂H), 7.95 (d, ³J(H,H) = 8.8 Hz, 12H; C₂H), 7.97 (s, 24H; C₁^{6,7}H), 10.06 (s, 6H; CHO); ¹³C {¹H} NMR (CDCl₃): δ = 33.0 (d, ²J(C,P) = 13.6 Hz; CH₃NP₁), 121.6 (d, ³J(C,P) = 4.8 Hz; C₂), 122.2 (d, ³J(C,P) = 5.8 Hz; C₂), 123.3 (C₁), 124.8 (C₁), 128.5 (C₂), 130.7 (C₁), 132.5 (C₄), 137.5 (C₈), 138.9 (d, ³J(C,P) = 13.8 Hz; CH=N₍₀₎), 149.9 (C₄), 151.3 (d, ²J(C,P) = 7.9 Hz; C₀), 153.3 (d, ²J(C,P) = 7.9 Hz, C₁), 155.7 (C₁), 191.0 (CHO); IR (KBr): $\tilde{\nu}$ = 1699 cm⁻¹ (CHO); UV/Vis (CHCl₃): λ_{max} (ε) = 340 (157800), 444 nm (4100 m⁻¹ cm⁻¹); elemental analysis calcd (%) for C₁₀₂H₇₈N₁₈O₁₅P₄S₄ (2048.01): C 59.82, H 3.83, N 12.30; found C 60.00, H 3.93, N 12.35.

Dendrimer 5-G₁: 76% yield (0.28 g); ³¹P {¹H} NMR ([D₆]DMSO): δ = 15.2 (d, ²J(P₁,P₁) = 25.7 Hz; P₁), 60.6 (d, ²J(P₁,P₁) = 25.7 Hz; P₁), 77.9 (P₀); ¹H NMR ([D₆]DMSO): δ = 3.23 (d, ³J(H,P₁) = 8.8 Hz, 18H; CH₃NP₁), 3.32 (d, ³J(H,P₀) = 8.4 Hz, 9H; CH₃NP₀), 7.04 (d, ³J(H,H) = 8.4 Hz, 12H; HC₂), 7.50–7.90 (m, 51H; H_{arom}, CH=N), 7.73 (d, ³J(H,H) = 15.5 Hz, 12H; HC₂), 7.77 (d, ³J(H,H) = 15.5 Hz, 12H; HC₂), 7.88 (d, ³J(H,H) = 8.4 Hz, 12H; HC₂), 10.46 (brs, 6H; OH); ¹³C {¹H} NMR ([D₆]DMSO): δ = 33.9 (d, ²J(C,P₁) = 9.9 Hz; CH₃NP₁), 34.4 (d, ²J(C,P₀) = 8.2 Hz; CH₃NP₀), 117.2 (C₂), 123.7 (C₂), 126.1 (C₂), 127.4 (d, ³J(C,P₁) = 11.1 Hz; C₂), 127.9 (C₂), 129.9 (d, ³J(C,P₁) = 12.8 Hz; C₂), 130.2 (dd, ¹J(C,P₁) = 106.0 Hz, ³J(C,P₁) = 2.8 Hz; C₁), 130.5 (brd, ¹J(C,P₁) = 106.7 Hz; C₁), 133.4–134.2 (m; C₁, C₂, C₂), 135.3 (d, ³J(C,P₁) = 14.0 Hz; CH=N₍₂₎), 138.4 (m; CH=N₍₁₎), 139.7 (C₈), 140.5 (d, ⁴J(C,P) = 2 Hz; C₁), 140.6 (C₂), 152.5 (C₂), 162.2 (C₂); UV/Vis (DMSO): λ_{max} (ε) = 262 (97400), 324 (98500), 396 nm (165000 m⁻¹ cm⁻¹); elemental analysis calcd (%) for C₁₄₄H₁₃₂N₃₃O₆P₄S₄ (2765.9): C 62.53, H 4.81, N 16.71; found C 62.28, H 4.74, N 16.63.

Dendrimer 5-G₄: 67% yield (0.099 g); ³¹P {¹H} NMR ([D₈]THF): δ = 14.3 (d, ²J(P₄,P₄) = 26.5 Hz; P₄), 15.3 (brd, ²J(P,P) = 27.8 Hz; P₁, P₂, P₃), 59.8 (d, ²J(P₄,P₄) = 26.5 Hz; P₄), 59.9 (m; P₁, P₂, P₃), 76.7 (P₀); ¹H NMR ([D₈]THF): δ = 3.33 (brs, 279H; CH₃), 6.99 (d, ³J(H,H) = 7.8 Hz, 96H; HC₂), 7.30–8.20 (m, 819H; H_{arom}, CH=N), 7.84 (d, ³J(H,H) = 15.4 Hz, 96H; HC₂), 7.88 (d, ³J(H,H) = 15.4 Hz, 96H; HC₂), 9.23 (brs, 48H; OH); ¹³C {¹H} NMR

([D₈]THF): δ = 32.1 (d, ²J(C,P₄) = 10.8 Hz; CH₃NP₄), 32.5 (m; CH₃), 115.6 (C₂), 122.5 (C₂), 124.7 (C₂), 125.6 (m; C₁₋₄), 126.6 (C₂), 128.3 (d, ³J(C,P) = 11.8 Hz; C₁₋₄), 129.7 (brd, ¹J(C,P) = 106 Hz; C₄, C₁), 130.0 (brd, ¹J(C,P) = 107 Hz; C₂₋₃, C₂₋₃), 130.3 (brd, ¹J(C,P) = 106 Hz; C₄, C₁), 132.1 (m; C₁₋₄), 132.9 (brs; C₁₋₄, C₁₋₄, CH=N₍₅₎), 138.2 (m; CH=N₍₁₋₄₎), 139.2 (s; C₈, C₁), 141.0 (brs; C₂₋₄), 146.3 (C₂), 151.8 (C₂), 160.9 (C₂); UV/Vis (DMSO): λ_{max} (ε) = 262 (1296000), 340 (1520000), 396 nm (1380000 m⁻¹ cm⁻¹); elemental analysis calcd (%) for C₁₅₇₂H₁₄₃₄N₃₂₇O₄₈P₉₁S₄₆ (29968): C 63.00, H 4.82, N 15.28; found C 62.89, H 4.88, N 15.11.

Dendrimer 6-G₂: 99% yield (1.16 g); ³¹P {¹H} NMR (CDCl₃): δ = 52.5 (P₀), 61.6 (P₁), 63.1 (P₂); ¹H NMR (CDCl₃): δ = 3.41 (d, ³J(H,P) = 10.2 Hz, 9H; CH₃NP₁), 3.50 (d, ³J(H,P) = 13.6 Hz, 18H; CH₃NP₂), 7.30 (d, ³J(H,H) = 8.7 Hz, 6H; C₂H), 7.38 (dd, ³J(H,H) = 8.8 Hz, ³J(H,P) = 1.3 Hz, 12H; C₂H), 7.65 (s, 3H; CH=N₍₀₎), 7.72 (s, 6H; CH=N₍₁₎), 7.77 (d, ³J(H,H) = 8.7 Hz, 6H; C₂H), 7.85–7.94 (m, 36H; C₁^{6,7}H); ¹³C {¹H} NMR (CDCl₃): δ = 31.9 (d, ²J(C,P) = 13.8 Hz; CH₃NP₂), 33.1 (d, ²J(C,P) = 12.2 Hz; CH₃NP₁), 121.6 (d, ³J(C,P) = 4.6 Hz; C₂), 122.1 (d, ³J(C,P) = 5.2 Hz; C₂), 123.4 (C₁), 124.5 (C₁), 128.2 (C₁), 128.5 (C₁), 132.6 (C₄), 136.4 (C₈), 138.9 (d, ³J(C,P) = 13.8 Hz; CH=N₍₀₎), 140.7 (d, ³J(C,P) = 18.3 Hz; CH=N₍₁₎), 149.9 (C₄), 151.3 (d, ²J(C,P) = 7.6 Hz; C₀), 152.8 (d, ²J(C,P) = 7.7 Hz; C₁), 153.1 (C₁); UV/Vis (CHCl₃): λ_{max} (ε) = 360 nm (223200 m⁻¹ cm⁻¹); elemental analysis calcd (%) for C₁₀₈H₉₆Cl₁₂N₃₀O₉P₁₀S₁₀ (3013.98): C 43.03, H 3.21, N 13.94; found C 42.95, H 3.32, N 13.85.

Dendrimer 6-G₂: 93% yield (0.33 g); ³¹P {¹H} NMR (CDCl₃): δ = 52.5 (P₀), 60.4 (P₂), 61.7 (P₁); ¹H NMR (CDCl₃): δ = 3.42 (d, ³J(H,P) = 10.6 Hz, 27H; CH₃NP_{1,2}), 7.32 (d, ³J(H,H) = 8.2 Hz, 6H; C₂H), 7.39 (d, ³J(H,H) = 8.0 Hz, 36H; C₂H), 7.70 (s, 9H; CH=N_(0,1)), 7.78 (d, ³J(H,H) = 8.2 Hz, 6H; C₂H), 7.86 (d, ³J(H,H) = 8.0 Hz, 24H; C₂H), 7.84–7.93 (m, 36H; C₁^{6,7}H), 9.93 (s, 12H; CHO); ¹³C {¹H} NMR (CDCl₃): δ = 33.1 (d, ²J(C,P) = 13.8 Hz; CH₃NP_{1,2}), 121.6 (d, ³J(C,P) = 3.8 Hz; C₂), 122.0 (d, ³J(C,P) = 5.3 Hz; C₂), 122.1 (d, ³J(C,P) = 5.3 Hz; C₂), 123.4 (C₁), 124.5 (C₁), 127.8 (C₁), 128.5 (C₂), 131.5 (C₂), 132.6 (C₀), 133.7 (C₂), 136.8 (C₈), 139.0 (d, ³J(C,P) = 13.9 Hz; CH=N₍₀₎), 139.7 (d, ³J(C,P) = 13.8 Hz; CH=N₍₁₎), 150.0 (C₄), 151.3 (d, ²J(C,P) = 7.7 Hz; C₀), 152.7 (d, ²J(C,P) = 7.0 Hz; C₁), 153.0 (C₁), 155.1 (d, ²J(C,P) = 6.1 Hz; C₂), 190.7 (CHO); IR (KBr): $\tilde{\nu}$ = 1702 cm⁻¹ (CHO); UV/Vis (CHCl₃): λ_{max} (ε) = 258 (269700), 362 (198600), 442 nm (10100 m⁻¹ cm⁻¹); elemental analysis calcd (%) for C₁₉₂H₁₅₆N₃₀O₃₃P₁₀S₁₀ (4041.92): C 57.05, H 3.89, N 10.39; found C 57.17, H 4.05, N 10.17.

Dendrimer 6-G₃: 85% yield (0.29 g); ³¹P {¹H} NMR (CDCl₃): δ = 52.5 (P₀), 61.7 (P_{1,2}), 63.6 (P₃); ¹H NMR (CDCl₃): δ = 3.43 (brd, ³J(H,P) = 13.9 Hz, 63H; CH₃NP_{1,2,3}), 7.29 (d, ³J(H,H) = 8.0 Hz, 30H; C₂H), 7.38 (d, ³J(H,H) = 8.6 Hz, 12H; C₂H), 7.63 (s, 21H; CH=N_(0,1,2)), 7.71 (d, ³J(H,H) = 8.0 Hz, 24H; C₂H), 7.68–7.93 (m, 42H; H_{arom}); ¹³C {¹H} NMR (CDCl₃): δ = 31.7 (d, ²J(C,P) = 13.1 Hz; CH₃NP₃), 33.0 (d, ²J(C,P) = 12.6 Hz; CH₃NP₂), 32.1 (d, ²J(C,P) = 12.6 Hz; CH₃NP₁), 121.5 (d, ³J(C,P) = 4.4 Hz; C₂), 121.8 (d, ³J(C,P) = 4.4 Hz; C₂), 121.9 (d, ³J(C,P) = 5.1 Hz; C₂), 123.2 (C₁), 124.3 (C₁), 128.0 (C₁), 128.2 (C₂), 128.6 (C₂), 131.4 (C₄), 132.4 (C₀), 136.9 (C₈), 138.9 (d, ³J(C,P) = 15.6 Hz; CH=N_(0,1)), 140.5 (d, ³J(C,P) = 18.6 Hz; CH=N₍₂₎), 149.8 (C₄), 151.2 (d, ²J(C,P) = 6.2 Hz; C₀), 151.7 (d, ²J(C,P) = 6.8 Hz; C₂), 152.5 (d, ²J(C,P) = 7.1 Hz; C₁), 152.7 (C₁); UV/Vis (CHCl₃): λ_{max} (ε) = 286 (384500), 366 (194400), 444 nm (12100 m⁻¹ cm⁻¹); elemental analysis calcd (%) for C₂₀₄H₁₉₂Cl₂₄N₅₄O₂₁P₂₂S₂₂ (5973.86): C 41.01, H 3.23, N 12.66; found C 41.32, H 3.54, N 12.76.

Dendrimer 6-G₃: 86% yield (0.30 g); ³¹P {¹H} NMR (CDCl₃): δ = 52.6 (P₀), 60.5 (P₃), 61.9 (P_{1,2}); ¹H NMR (CDCl₃): δ = 3.37 (brd, ³J(H,P) = 10.3 Hz, 63H; CH₃NP_{1,2,3}), 7.34 (d, ³J(H,H) = 7.7 Hz, 90H; C_{0,1,2,3}H), 7.62 (s, 12H; CH=N₍₂₎), 7.66 (s, 9H; CH=N_(0,1)), 7.83 (d, ³J(H,H) = 7.7 Hz, 48H; C₂H), 7.70–7.93 (m, 66H; H_{arom}), 9.91 (s, 24H; CHO); ¹³C {¹H} NMR (CDCl₃): δ = 32.8 (d, ²J(C,P) = 13.4 Hz; CH₃NP₃), 32.9 (d, ²J(C,P) = 12.7 Hz; CH₃NP_{1,2}), 121.8 (d, ³J(C,P) = 4.8 Hz; C₂), 123.2 (C₁), 124.3 (C₁), 127.6 (C₁), 128.2 (C₂), 128.4 (C₂), 131.3 (C₂), 131.7 (C₂), 132.4 (C₀), 133.5 (C₄), 136.9 (C₈), 139.0 (d, ³J(C,P) = 13.1 Hz; CH=N_(0,1)), 139.4 (d, ³J(C,P) = 14.2 Hz; CH=N₍₂₎), 149.8 (C₄), 151.2 (d, ²J(C,P) = 6.1 Hz; C₀), 151.3 (d, ²J(C,P) = 6.5 Hz; C₂), 151.4 (d, ²J(C,P) = 7.3 Hz; C₂), 152.6 (d, ²J(C,P) = 6.9 Hz; C₁), 152.7 (C₁), 190.6 (CHO); IR (KBr): $\tilde{\nu}$ = 1702 cm⁻¹ (CHO); UV/Vis (CHCl₃): λ_{max} (ε) = 262 (525400), 366 nm (204000 m⁻¹ cm⁻¹); elemental analysis calcd (%) for C₃₇₂H₃₁₂N₅₄O₆₉P₂₂S₂₂ (8029.75): C 55.64, H 3.91, N 9.42; found C 55.79, H 4.25, N 9.49.

Dendrimer 7-G₂: 90% yield (0.20 g); ³¹P {¹H} NMR (CDCl₃): δ = 52.5 (P₀), 61.0 (P₂), 61.6 (P₁); ¹H NMR (CDCl₃): δ = 3.42 (m, 27H; CH₃NP_{1,2}), 7.40

(m, 42H; C_{0,1,2}H), 7.70–8.08 (m, 123H; H_{arom}, CH=N_(0,1)), 10.05 (s, 12H; CHO); ¹³C {¹H} NMR (CDCl₃): δ = 33.1 (d, ³J(C,P) = 12.2 Hz; CH₃NP₁), 33.2 (d, ²J(C,P) = 13.3 Hz; CH₃NP₂), 121.6 (d, ³J(C,P) = 4.5 Hz; C₀), 122.2 (d, ³J(C,P) = 5.3 Hz; C_{1,2}), 123.3 (C₃), 123.4 (C₄), 124.4 (C₅), 124.8 (C₆), 127.8 (C₇), 128.5 (C₈), 130.7 (C₉), 132.6 (C₁₀), 136.9 (C₁₁), 137.5 (C₁₂), 138.9 (d, ³J(C,P) = 19.7 Hz; CH=N₍₀₎), 139.3 (d, ³J(C,P) = 13.9 Hz; CH=N₍₁₎), 149.9 (C₁₃), 149.9 (C₁₄), 151.3 (d, ²J(C,P) = 7.9 Hz; C₀), 152.7 (d, ²J(C,P) = 6.1 Hz; C₁), 152.9 (C₂), 153.3 (d, ²J(C,P) = 6.5 Hz; C₂), 155.7 (C₃), 191.6 (CHO); IR (KBr): ν̄ = 1696 cm⁻¹ (CHO); UV/Vis (CHCl₃): λ_{max} (ε) = 348 (498 600), 448 nm (39 000 M⁻¹ cm⁻¹); elemental analysis calcd (%) for C₂₆₄H₂₀₄N₅₄O₃₃P₁₀S₁₀ (5291.26): C 59.92, H 3.88, N 14.29; found C 59.83, H 3.65, N 14.02.

Dendrimer 7-G₃: 86% yield (0.31 g); ³¹P {¹H} NMR (CDCl₃): δ = 52.4 (P₀), 61.2 (P₂), 61.6 (P₁), 63.1 (P₃); ¹H NMR (CDCl₃): δ = 3.46 (m, 63H; CH₃NP_{1,2,3}), 7.32 (m, 42H; C_{0,1,2}H), 7.60–8.00 (m, 135H; H_{arom}, CH=N_(0,1,2)); ¹³C {¹H} NMR (CDCl₃): δ = 31.9 (d, ²J(C,P) = 13.7 Hz; CH₃NP₃), 33.1 (d, ²J(C,P) = 12.0 Hz; CH₃NP₁), 33.2 (d, ²J(C,P) = 13.5 Hz; CH₃NP₂), 121.7 (d, ³J(C,P) = 3.5 Hz; C₀), 122.1 (d, ³J(C,P) = 3.9 Hz; C_{1,2}), 123.4 (C_{3,2}), 124.5 (C_{6,2}), 127.8 (C₁), 128.2 (C₂), 128.6 (C₃), 132.6 (C₄), 136.4 (C₈), 137.0 (C₈), 139.2 (d, ³J(C,P) = 14.2 Hz; CH=N₍₀₎), 139.4 (d, ³J(C,P) = 13.8 Hz; CH=N₍₁₎), 140.1 (d, ³J(C,P) = 19.0 Hz; CH=N₍₂₎), 149.9 (C_{1,2}), 151.2 (d, ²J(C,P) = 7.7 Hz; C₀), 152.7 (d, ²J(C,P) = 6.1 Hz; C₁), 152.8 (d, ²J(C,P) = 7.3 Hz; C₂), 152.9 (C₃), 153.1 (C₃); UV/Vis (CHCl₃): λ_{max} (ε) = 362 (648 000), 442 nm (37 500 M⁻¹ cm⁻¹); elemental analysis calcd (%) for C₂₇₆H₂₄₀Cl₂₄N₇₈O₂₁P₂₂S₂₂ (7223.19): C 45.89, H 3.34, N 15.12; found C 46.02, H 3.57, N 15.35.

Dendrimer 7-G₄: 85% yield (0.27 g); ³¹P {¹H} NMR (CDCl₃): δ = 52.5 (P₀), 61.0 (P₃), 61.5 (P_{1,2}); ¹H NMR (CDCl₃): δ = 3.43 (m, CH₃NP_{1,2,3}; 63H), 7.42 (m, 90H; C_{0,1,2,3}H), 7.50–8.20 (m, 279H; H_{arom}, CH=N_(0,1,2)), 10.01 (brs, 24H; CHO); ¹³C {¹H} NMR (CDCl₃): δ = 33.2 (brd, ²J(C,P) = 13.4 Hz; CH₃NP_{1,2,3}), 121.6 (brs; C₀), 122.1 (brs; C_{1,2,3}), 123.3 (C_{3,3}), 123.4 (C₃), 124.4 (C_{6,2}), 124.8 (C₆), 127.8 (C_{1,2}), 128.5 (C₃), 130.7 (C₁), 132.5 (C₄), 136.9 (C₈), 137.0 (C₈), 137.4 (C₈), 138.9 (d, ³J(C,P) = 13.7 Hz; CH=N₍₀₎), 139.2 (d, ³J(C,P) = 13.8 Hz; CH=N₍₁₎), 139.3 (d, ³J(C,P) = 12.4 Hz; CH=N₍₂₎), 149.6 (C₁), 149.8 (C₄), 150.0 (C₄), 151.3 (brs; C₀), 152.7 (d, ²J(C,P) = 7.1 Hz; C_{1,2}), 152.8 (C_{1,2}), 153.3 (d, ²J(C,P) = 7.4 Hz; C₃), 155.6 (C₃), 191.6 (CHO); IR (KBr): ν̄ = 1698 cm⁻¹ (CHO); UV/Vis (CHCl₃): λ_{max} (ε) = 352 (1155 000), 460 nm (74 700 M⁻¹ cm⁻¹); elemental analysis calcd (%) for C₃₈₈H₄₅₆N₁₂₆O₆₉P₂₂S₂₂ (11 777.75): C 59.96, H 3.90, N 14.98; found C 60.0, H 3.99, N 15.23.

Dendrimer 8-G₀: 95% yield (0.21 g); ³¹P {¹H} NMR (CDCl₃): δ = 8.4 (P₀); ¹H NMR (CDCl₃): δ = 7.20 (d, ³J(H,H) = 7.9 Hz, 12H; C₀H), 7.80 (d, ³J(H,H) = 7.9 Hz, 12H; C₀H), 7.88 (brs, 24H; C₀H), 10.05 (s, 6H; CHO); ¹³C {¹H} NMR (CDCl₃): δ = 121.5 (C₀), 123.3 (C₀), 124.7 (C₀), 130.5 (C₀), 137.5 (C₀), 149.8 (C₀), 152.8 (d, ²J(C,P) = 6.9 Hz; C₀), 155.5 (C₀), 191.4 (CHO); IR (KBr): ν̄ = 1700 cm⁻¹ (CHO); UV/Vis (CHCl₃): λ_{max} (ε) = 336 (151 200), 434 nm (5700 M⁻¹ cm⁻¹); elemental analysis calcd (%) for C₇₈H₅₄N₁₅O₁₂P₃ (1486.30): C 63.03, H 3.66, N 14.13; found C 63.22, H 3.98, N 14.26.

Dendrimer 8-G₁: 98% yield (0.59 g); ³¹P {¹H} NMR (CDCl₃): δ = 8.7 (P₀), 62.6 (P₁); ¹H NMR (CDCl₃): δ = 3.51 (d, ³J(H,P) = 13.7 Hz, 18H; CH₃NP₁), 7.17 (d, ³J(H,H) = 8.7 Hz, 12H; C₀H), 7.69 (s, 6H; CH=N₍₀₎), 7.78 (d, ³J(H,H) = 8.7 Hz, 12H; C₀H), 7.80 (d, ³J(H,H) = 7.0 Hz, 24H; C₀H); ¹³C {¹H} NMR (CDCl₃): δ = 32.5 (d, ²J(C,P) = 12.3 Hz; CH₃NP₁), 121.5 (C₀), 123.4 (C₀), 124.5 (C₀), 128.1 (C₀), 136.3 (C₀), 140.8 (d, ³J(C,P) = 19.5 Hz; CH=N₍₀₎), 149.9 (C₀), 152.4 (brs; C₀), 153.1 (C₀); UV/Vis (CHCl₃): λ_{max} (ε) = 356 (225 600), 440 nm (9800 M⁻¹ cm⁻¹); elemental analysis calcd (%) for C₈₄H₇₂Cl₁₂N₂₇O₆P₉S₆ (2452.27): C 41.14, H 2.95, N 15.42; found C 41.30, H 3.20, N 15.31.

Dendrimer 8-G₁: 85% yield (0.82 g); ³¹P {¹H} NMR (CDCl₃): δ = 8.6 (P₀), 61.2 (P₁); ¹H NMR (CDCl₃): δ = 3.42 (d, ³J(H,P) = 10.5 Hz, 18H; CH₃NP₁), 7.20 (d, ³J(H,H) = 8.9 Hz, 12H; C₀H), 7.41 (dd, ³J(H,H) = 8.7 Hz, ⁴J(H,P) = 1.3 Hz, 24H; C₀H), 7.72 (s, 6H; CH=N₍₀₎), 7.82 (d, ³J(H,H) = 8.7 Hz, 24H; C₀H), 7.90 (d, ³J(H,H) = 8.9 Hz, 12H; C₀H), 7.91 (s, 24H; C₀H), 7.95 (brs, 48H; C₀H), 10.04 (s, 12H; CHO); ¹³C {¹H} NMR (CDCl₃): δ = 33.2 (d, ²J(C,P) = 12.0 Hz; CH₃NP₁), 121.6 (C₀), 122.1 (d, ³J(C,P) = 5.5 Hz; C₁), 123.3 (C₁), 123.5 (C₀), 124.3 (C₀), 124.8 (C₁), 127.8 (C₀), 130.6 (C₁), 137.0 (C₀), 137.5 (C₁), 139.4 (d, ³J(C,P) = 13.8 Hz; CH=N₍₀₎), 149.9 (C_{1,1}), 152.5 (brs; C₀), 152.8 (C₀), 153.2 (d, ²J(C,P) = 7.8 Hz; C₁), 155.6 (C₁), 191.5 (CHO); IR (KBr): ν̄ = 1699 cm⁻¹ (CHO);

UV/Vis (CHCl₃): λ_{max} (ε) = 348 (498 600), 440 nm (22 300 M⁻¹ cm⁻¹); elemental analysis calcd (%) for C₂₄₀H₁₈₀N₅₁O₃₀P₉S₆ (4729.55): C 60.95, H 3.83, N 15.10; found C 61.12, H 3.65, N 14.98.

Dendrimer 8-G₂: 99% yield (0.67 g); ³¹P {¹H} NMR (CDCl₃): δ = 8.7 (P₀), 61.3 (P₁), 63.0 (P₂); ¹H NMR (CDCl₃): δ = 3.39 (d, ³J(H,P) = 10.1 Hz, 18H; CH₃NP₁), 3.47 (d, ³J(H,P) = 13.3 Hz, 36H; CH₃NP₂), 7.17 (d, ³J(H,H) = 7.6 Hz, 12H; C₀H), 7.40 (d, ³J(H,H) = 7.1 Hz, 24H; C₀H), 7.68 (s, 18H; CH=N_(0,1)), 7.79–7.94 (m, 108H; C_{0,1}H); ¹³C {¹H} NMR (CDCl₃): δ = 31.9 (d, ²J(C,P) = 12.4 Hz; CH₃NP₂), 33.2 (d, ²J(C,P) = 13.4 Hz; CH₃NP₁), 121.6 (C₀), 122.1 (d, ³J(C,P) = 3.9 Hz; C₁), 123.4 (C₁), 123.6 (C₀), 124.5 (C_{0,1}), 127.7 (C₀), 128.1 (C₁), 136.4 (C₁), 137.1 (C₀), 139.2 (d, ³J(C,P) = 14.1 Hz; CH=N₍₀₎), 140.7 (d, ³J(C,P) = 17.9 Hz; CH=N₍₁₎), 149.9 (C_{0,1}), 152.4 (brs; C₀), 152.8 (d, ²J(C,P) = 8.6 Hz; C₁), 152.9 (C₀), 153.1 (C₁); UV/Vis (CHCl₃): λ_{max} (ε) = 362 (662 400), 446 nm (35 600 M⁻¹ cm⁻¹); elemental analysis calcd (%) for C₂₅₂H₂₁₆Cl₂₄N₇₅O₁₈P₂₁S₁₈ (6661.48): C 45.43, H 3.26, N 15.77; found C 45.58, H 3.37, N 15.55.

Dendrimer 8-G₂: 85% yield (0.56 g); ³¹P {¹H} NMR (CDCl₃): δ = 8.6 (P₀), 61.1 (P₂), 61.5 (P₁); ¹H NMR (CDCl₃): δ = 3.41 (brs, 54H; CH₃NP_{1,2}), 7.39 (brs, 84H; C_{0,1,2}H), 7.50–8.20 (m, 270H; H_{arom}, CH=N_(0,1)), 9.98 (s, 24H; CHO); ¹³C {¹H} NMR (CDCl₃): δ = 33.2 (d, ²J(C,P) = 12.7 Hz; CH₃NP_{1,2}), 121.5 (C₀), 122.1 (d, ³J(C,P) = 3.3 Hz; C_{1,2}), 123.3 (C₂), 123.4 (C_{0,1}), 124.4 (C_{0,1}), 124.8 (C₀), 127.8 (C_{0,1}), 130.6 (C₂), 137.0 (C₁), 137.1 (C₀), 137.7 (C₀), 139.3 (d, ³J(C,P) = 13.7 Hz; CH=N_(0,1)), 149.8 (C_{0,1,2}), 152.4 (brs; C₀), 152.7 (d, ²J(C,P) = 8.7 Hz; C₁), 152.8 (C_{0,1}), 153.3 (d, ²J(C,P) = 7.0 Hz; C₂), 155.6 (C₂), 191.6 (CHO); IR (KBr): ν̄ = 1697 cm⁻¹ (CHO); UV/Vis (CHCl₃): λ_{max} (ε) = 352 nm (1176 000 M⁻¹ cm⁻¹); elemental analysis calcd (%) for C₃₆₄H₄₃₂N₁₂₃O₆₆P₂₁S₁₈ (11 216.04): C 60.39, H 3.88, N 15.36; found C 60.28, H 3.95, N 15.28.

Acknowledgements

Thanks are due to the CNRS (France) for financial support and to the foundation Ramon Areces (Spain) for a grant to one of us (RMS).

- [1] For reviews, see for example: a) D. A. Tomalia, A. M. Naylor, W. A. Goddard III, *Angew. Chem.* **1990**, *102*, 119; *Angew. Chem. Int. Ed. Engl.* **1990**, *29*, 138; b) D. A. Tomalia, H. D. Durst, *Top. Curr. Chem.* **1993**, *165*, 193–313; *Supramolecular Chemistry I* (Ed.: E. Weber), Springer, Berlin, **1993**, pp. 193–313; c) G. R. Newkome, C. N. Moorefield, F. Vögtle, *Dendritic Molecules*, VCH, Weinheim, **1996**; d) F. Zeng, S. C. Zimmerman, *Chem. Rev.* **1997**, *97*, 1681; e) A. Archut, F. Vögtle, *Chem. Soc. Rev.* **1998**, *27*, 233; f) H. F. Chow, T. K. K. Mong, M. F. Nongrum, C. W. Wan, *Tetrahedron* **1998**, *54*, 8543; g) M. Fischer, F. Vögtle, *Angew. Chem.* **1999**, *111*, 934; *Angew. Chem. Int. Ed.* **1999**, *38*, 884; h) A. W. Bosman, H. M. Janssen, E. W. Meijer, *Chem. Rev.* **1999**, *99*, 1665; i) J. P. Majoral, A. M. Caminade, *Chem. Rev.* **1999**, *99*, 845.
- [2] S. Hecht, J. M. J. Fréchet, *Angew. Chem.* **2001**, *113*, 76; *Angew. Chem. Int. Ed.* **2001**, *40*, 74.
- [3] a) N. Launay, A. M. Caminade, R. Lahana, J. P. Majoral, *Angew. Chem.* **1994**, *106*, 1682; *Angew. Chem. Int. Ed. Engl.* **1994**, *33*, 1589; b) N. Launay, A. M. Caminade, J. P. Majoral, *J. Am. Chem. Soc.* **1995**, *117*, 3282; c) C. Galliot, D. Prévôté, A. M. Caminade, J. P. Majoral, *J. Am. Chem. Soc.* **1995**, *117*, 5470; d) M. Slany, M. Bardají, M. J. Casanove, A. M. Caminade, J. P. Majoral, B. Chaudret, *J. Am. Chem. Soc.* **1995**, *117*, 9764; e) C. Larré, A. M. Caminade, J. P. Majoral, *Angew. Chem.* **1997**, *109*, 613; *Angew. Chem. Int. Ed. Engl.* **1997**, *36*, 596; f) C. Galliot, C. Larré, A. M. Caminade, J. P. Majoral, *Science* **1997**, *277*, 1981; g) C. Larré, B. Donnadieu, A. M. Caminade, J. P. Majoral, *J. Am. Chem. Soc.* **1998**, *120*, 4029; h) C. Larré, D. Bressolles, C. Turrin, B. Donnadieu, A. M. Caminade, J. P. Majoral, *J. Am. Chem. Soc.* **1998**, *120*, 13070; i) V. Maraval, R. Laurent, B. Donnadieu, M. Mauzac, A. M. Caminade, J. P. Majoral, *J. Am. Chem. Soc.* **2000**, *122*, 2499; j) M. K. Boggiano, G. J. A. A. Soler-Illia, L. Rozes, C. Sanchez, C. O. Turrin, A. M. Caminade, J. P. Majoral, *Angew. Chem.* **2000**, *112*, 4419; *Angew. Chem. Int. Ed.* **2000**, *39*, 4249; k) F. Le Derf, E. Levillain, G. Trippé, A. Gorgues, M. Sallé, R. M. Sebastián, A. M. Caminade, J. P. Majoral, *Angew. Chem.* **2001**, *113*, 230; *Angew. Chem. Int. Ed.*

- 2001**, 40, 224; l) L. Brauge, G. Magro, A. M. Caminade, J. P. Majoral, *J. Am. Chem. Soc.* **2001**, 123, 6698.
- [4] M. L. Lartigue, B. Donnadieu, C. Galliot, A. M. Caminade, J. P. Majoral, J. P. Fayet, *Macromolecules* **1997**, 30, 7335.
- [5] M. L. Lartigue, A. M. Caminade, J. P. Majoral, *Tetrahedron: Asymmetry* **1997**, 8, 2697.
- [6] C. O. Turrin, J. Chiffre, D. de Montauzon, J. C. Daran, A. M. Caminade, E. Manoury, G. Balavoine, J. P. Majoral, *Macromolecules* **2000**, 33, 7328.
- [7] V. Maraval, R. Laurent, A. M. Caminade, J. P. Majoral, *Organometallics* **2000**, 19, 4025.
- [8] G. Schmid, W. Meyer-Zaika, R. Pugin, T. Sawitowski, J. P. Majoral, A. M. Caminade, C. O. Turrin, *Chem. Eur. J.* **2000**, 6, 1693.
- [9] C. Loup, M. A. Zanta, A. M. Caminade, J. P. Majoral, B. Meunier, *Chem. Eur. J.* **1999**, 5, 3644.
- [10] G. S. Kumar, D. C. Neckers, *Chem. Rev.* **1989**, 89, 1915.
- [11] a) H. B. Meckelburger, K. Rissanen, F. Vögtle, *Chem. Ber.* **1993**, 126, 1161; b) R. Moors, F. Vögtle, *Adv. Dendritic Macromol.* **1995**, 2, 41; c) A. Archut, G. C. Azzellini, V. Balzani, L. DeCola, F. Vögtle, *J. Am. Chem. Soc.* **1998**, 120, 12187; d) A. Archut, F. Vögtle, L. DeCola, G. C. Azzellini, V. Balzani, P. S. Ramanujam, R. H. Berg, *Chem. Eur. J.* **1998**, 4, 699; e) A. Archut, F. Vögtle, *Chem. Soc. Rev.* **1998**, 27, 233; f) S. Li, D. V. McGrath, *J. Am. Chem. Soc.* **2000**, 122, 6795.
- [12] a) D. L. Jiang, T. Aida, *Nature* **1997**, 388, 454; b) T. Aida, D. L. Jiang, E. Yashima, Y. Okamoto, *Thin Solid Films* **1998**, 331, 254; c) Y. Wakabayashi, M. Tokeshi, D. L. Jiang, T. Aida, T. Kitamori, *J. Lumin.* **1999**, 83–84, 313; d) S. Tanaka, S. Itoh, N. Kurita, *Chem. Phys. Lett.* **2000**, 323, 407.
- [13] a) D. M. Junge, D. V. McGrath, *Chem. Commun.* **1997**, 857; b) D. M. Junge, D. V. McGrath, *Polym. Mater. Sci. Eng.* **1997**, 77, 79; c) M. Hashemzadeh, D. V. McGrath, *Polym. Prepr.* **1998**, 39, 338; d) D. M. Junge, D. V. McGrath, *Polym. Prepr.* **1998**, 39, 340; e) D. V. McGrath, D. M. Junge, J. R. McElhanon, M. Hashemzadeh, *Polym. Prepr.* **1998**, 39, 281; f) S. Li, S. Sikder, D. V. McGrath, *Polym. Prepr.* **1999**, 40, 267; g) D. V. McGrath, D. M. Junge, *Macromol. Symp.* **1999**, 137, 57; h) D. V. McGrath, D. M. Junge, *Polym. Mater. Sci. Eng.* **1999**, 80, 62; i) D. V. McGrath, D. M. Junge, A. Chen, G. D'Ambruoso, *Mater. Res. Soc. Symp. Proc.* **1999**, 543, 319; j) L. Liao, D. V. McGrath, *Polym. Prepr.* **2000**, 41, 870.
- [14] a) T. Nagasaki, A. Noguchi, T. Matsumoto, S. Tamagaki, K. Ogino, *An. Quim. Int. Ed.* **1997**, 93, 341; b) T. Nagasaki, S. Tamagaki, K. Ogino, *Chem. Lett.* **1997**, 717.
- [15] a) S. Yokoyama, T. Nakahama, A. Otomo, S. Mashiko, *Chem. Lett.* **1997**, 1137; b) S. Yokoyama, T. Nakahama, S. Mashiko, *Mol. Cryst. Liq. Cryst.* **1997**, 294, 19; c) S. Yokoyama, T. Nakahama, A. Otomo, S. Mashiko, *Thin Solid Films* **1998**, 331, 248; d) S. Yokoyama, S. Mashiko, *Mater. Res. Soc. Symp. Proc.* **1998**, 488, 765; e) S. Yokoyama, T. Nakahama, A. Otomo, S. Mashiko, *J. Am. Chem. Soc.* **2000**, 122, 3174.
- [16] D. M. Junge, D. V. McGrath, *J. Am. Chem. Soc.* **1999**, 121, 4912.
- [17] *Macromol. Symp.* **1999**, 137, 1–165 (whole issue).
- [18] a) M. Negishi, O. Tsutsumi, T. Ikeda, T. Hiyama, J. Kawamura, M. Aizawa, S. Takehara, *Chem. Lett.* **1996**, 319; b) S. Takehara, H. Takasu, T. Hiyama, T. Ikeda, (Jpn Kokai Tokkyo Koho) JP09241230, 09.16.1997.
- [19] R. M. Sebastián, G. Magro, A. M. Caminade, J. P. Majoral, *Tetrahedron* **2000**, 56, 6269.
- [20] A dendrimer with 32 azo end groups^[11c, 11d] and a dendrimer with 60 azo derivatives within its skeleton, including 32 end groups^[14a, 14b] were the largest reported so far.
- [21] J. C. Blais, C. O. Turrin, A. M. Caminade, J. P. Majoral, *Anal. Chem.* **2000**, 72, 5097.
- [22] a) M. L. Lartigue, N. Launay, B. Donnadieu, A. M. Caminade, J. P. Majoral, *Bull. Soc. Chim. Fr.* **1997**, 134, 981; b) C. Larré, B. Donnadieu, A. M. Caminade, J. P. Majoral, *Chem. Eur. J.* **1998**, 4, 2031.
- [23] a) D. Tabak, H. Morawetz, *Macromolecules* **1970**, 3, 403; b) D. T. L. Chen, H. Morawetz, *Macromolecules* **1976**, 9, 463.
- [24] W. H. Wei, T. Tomohiro, M. Kodaka, H. Okumo, *J. Org. Chem.* **2000**, 65, 8979.
- [25] E. R. Talaty, J. C. Fargo, *Chem. Commun.* **1967**, 65.

Received: November 5, 2001 [F3657]